

In-Situ Interferometry Studies of the Drying and Swelling Kinetics of an Ultrathin Poly(*N*-isopropylacrylamide) Gel Film below and above Its Volume Phase Transition Temperature

Shuiqin Zhou and Chi Wu*

Department of Chemistry, The Chinese University of Hong Kong, Shatin, N.T., Hong Kong

Received November 13, 1995; Revised Manuscript Received April 25, 1996⁶

ABSTRACT: The temperature influence on the drying and swelling kinetics of ultrathin poly(*N*-isopropylacrylamide) gel film were studied by *in-situ* interferometry. The drying rate is greatly dependent on temperature. When $T \lesssim 31$ °C, the original gel film was swollen and contained more than 99% of water before drying. Our results showed that the initial drying rate was a constant. However, it became faster and faster toward the end of the drying. On the other hand, when $T \gtrsim 32$ °C, the gel film was in the collapsed state, but still contained ~70% of water, before drying. Three distinct drying processes were observed, namely, a very fast initial shrinking, a slow transition period, and a normal drying process similar to that of the gel film when $T \lesssim 31$ °C. As for the swelling process, it can be better described by the first-order kinetics developed by Li and Tanaka. The cooperative diffusion coefficient and the ratio of the shear modulus to the longitudinal modulus were determined from a least-squares fitting of the swelling experimental data according to the swelling equation for a large disk. A critical slowing down of the gel swelling for the thin film was observed in the range of 33–35 °C.

Introduction

Hydrogels, which can undergo a volume phase transition, have been extensively studied in recent years. A typical example is poly(*N*-isopropylacrylamide) (PNIPAM) gel, which has a sharp volume phase transition around the lower critical solution temperature (LCST) of linear PNIPAM chains; *i.e.*, PNIPAM gel swells when $T < \text{LCST}$, but collapses when $T > \text{LCST}$.¹ The volume change can be as large as $\sim 10^2$ times. Due to this special thermosensitivity, the PNIPAM gel might be utilized in various applications such as controlled drug delivery,^{2,3} molecular separation,⁴ and artificial muscle.⁵ Most of the past studies were focused on the swelling equilibrium. However, a better understanding of the swelling/shrinking kinetics of the PNIPAM gel is vitally important for its potential applications.

Few past studies have dealt with the swelling and shrinking kinetics of the PNIPAM gel in water.^{6–12} Tanaka *et al.*^{6,7} studied the swelling and shrinking kinetics of spherical-shaped PNIPAM gels by monitoring the changes in shape, size, and transient pattern with a microscope. They have shown that the motion of a polymer gel network during the swelling or shrinking process could be described by a collective diffusion equation. For a spherical gel of radius R , the swelling or shrinking rate was proportional to R^{-2} . The collective diffusion coefficient (D_c) diminished at the critical point of the volume phase transition. They also observed that the swelling and shrinking kinetics were much different. There were two distinct processes in the swelling: a fast initial process followed by a slower first-order process. On the other hand, a plateau was observed in the shrinking process, which was attributed to the dense surface layer formed during the initial shrinking. Hoffman *et al.*^{8,9} and Kim *et al.*^{10,11} characterized the shrinking kinetics of bulk disk PNIPAM gels by a conventional weighing method. They also found that the bulk gel did not collapse homogeneously, *i.e.*, the formation of a dense surface layer and water pocket retarded the shrinking kinetics.

To eliminate the inhomogeneous swelling and shrinking existing in a bulk gel and to simplify the kinetic

process, in this study we have studied an ultrathin PNIPAM gel film (~ 60 μm) by *in-situ* interferometry. The cooperative diffusion coefficient and the ratio of the shear modulus to the longitudinal modulus were determined on the basis of the following theory developed by Li and Tanaka.¹²

Theoretical Background

Swelling and Shrinking Kinetics. The swelling phenomena and its kinetics have been long studied. The swelling kinetics of a spherical gel was recently formulated by Tanaka and Fillmore on the basis of a cooperative diffusion theory,¹³ wherein the shear modulus was considered to be negligible in comparison with the osmotic compressive modulus. By including a nonnegligible shear modulus, Peters and Candau¹⁴ developed a general model to characterize the swelling kinetics of spherical, cylindrical, and disklike polymer gels. Later, Li and Tanaka¹² proposed a two-process mechanism after realizing that neither gel swelling nor shrinking can be considered to be a pure diffusion process. They predicted that the shear modulus (M_{shear}) is related to the net osmotic modulus (M_{os}) and the osmotic bulk modulus (K_{bulk}) by¹²

$$R = \frac{M_{\text{shear}}}{M_{\text{os}}} = \frac{M_{\text{shear}}}{K_{\text{bulk}} + \frac{4}{3}M_{\text{shear}}} \quad (1)$$

According to Li and Tanaka, the swelling or shrinking follows

$$\frac{W_{\infty} - W}{W_{\infty}} = \sum_{n=1}^{\infty} B_n \exp(-t/\tau_n) \quad (2)$$

where W and W_{∞} are the solvent uptake at time t and infinite time (*i.e.*, at equilibrium), respectively; $[(W_{\infty} - W)/W_{\infty}]$, the relative swelling capacity at time t ; B_n , a complicated function of R ; and τ_n , the relaxation time related to the n th mode. When $t \gg 1$ or $\tau_1 \gg \tau_n$ ($n \geq 2$) or $B_1 \gg B_n$ ($n \geq 2$), all high-order terms ($n \geq 2$) in eq 2 can be dropped. In this case, the swelling and shrinking follows a first-order kinetics, *i.e.*,

$$\ln\left(\frac{W_{\infty} - W}{W_{\infty}}\right) = \ln B_1 - t/\tau_1 \quad (3)$$

where B_1 is related to R by¹²

* Abstract published in *Advance ACS Abstracts*, June 1, 1996.

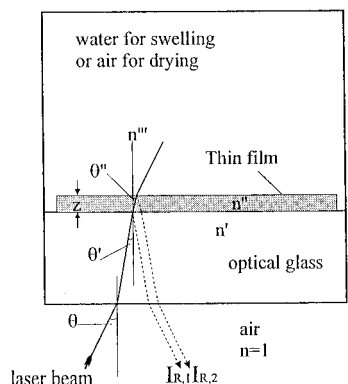


Figure 1. Schematic of the *in-situ* interferometer for measuring the ultrathin gel film thickness change, where a Nd-YAG solid laser ($\lambda_0 = 532$ nm) was used as the light source and the two reflected light beams were interfered at a photodiode to produce a voltage signal (V). The angle θ has been enlarged for a clear view. In our present setup, $\theta \approx 0$, $\theta' \approx 0$, and $\theta'' \approx 0$.

$$B_1 = \frac{2(3 - 4R)}{\alpha_1^2 - (4R - 1)(3 - 4R)} \quad (4)$$

and τ_1 is related to the collective diffusion coefficient D_c by¹²

$$D_c = \frac{3Z_\infty^2}{\tau_1 \alpha_1^2} \quad (5)$$

with α_1 being a function of R , *i.e.*,

$$R = \frac{1}{4} \left[1 + \frac{\alpha_1 J_0(\alpha_1)}{J_1(\alpha_1)} \right] \quad (6)$$

and Z_∞ being the disk thickness in the final swelling equilibrium state, where J_0 and J_1 are the zeroth- and first-order Bessel functions. The t -dependence of $[(W_\infty - W)/W_\infty]$ can lead first to B_1 and τ_1 , and then to R and D_c on the basis of eqs 3–6.

In-Situ Interferometry. The basic principle is schematically shown in Figure 1. When laser light hits a thin film at an angle of θ' smaller than the critical angle, it will be reflected twice by the interfaces between the film and the surrounding mediums due to difference in the refractive index (n' , n'' , and n''' , respectively). The two reflected light beams ($I_{R,1}$ and $I_{R,2}$) have an optical path difference of $2n''z \cos(\theta'')$, with z being the film thickness (~ 10 – $100 \mu\text{m}$). The interference of these two reflected light beams at the detector leads to¹⁵

$$I = E_{R,1}^2 + E_{R,2}^2 + 2E_{R,1}E_{R,2} \cos \left[\frac{4\pi n''z \cos(\theta'')}{\lambda_0} \right] \quad (7)$$

where $E_{R,1}$ and $E_{R,2}$ are respectively the electric fields of $I_{R,1}$ and $I_{R,2}$ (*i.e.*, $I_{R,1} = E_{R,1}^2$ and $I_{R,2} = E_{R,2}^2$) and λ_0 is the laser wavelength in vacuum. If z is a function of time, the intensity I will vary with z between the minimum $(E_{R,1} - E_{R,2})^2$ and the maximum $(E_{R,1} + E_{R,2})^2$. In this way, the intensity variation can be used to monitor the film thickness change.

Experimental Section

Sample Preparation. PNIPAM gel is very sticky so that it is rather difficult to directly make an ultrathin gel film. Instead, we made a gel film from narrowly distributed spherical microgel particles with an average diameter of $\sim 0.4 \mu\text{m}$. The PNIPAM microgel particles were made by suspension polymerization. NIPAM (15.90 g), *N,N*-methylenebis(acrylamide) (BIS) (0.2835 g), and sodium dodecyl sulfate (SDS) (0.1130 g) were added to 500 mL of deionized water. The solution was heated to 70 °C and stirred at 200 rpm for 40

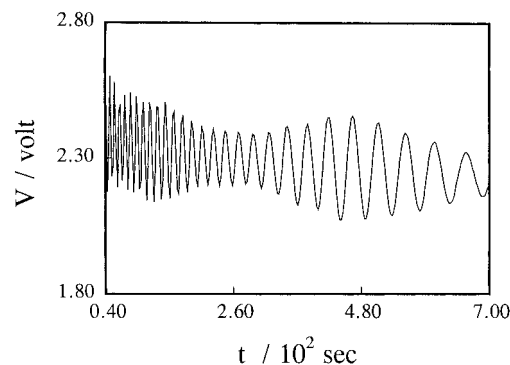


Figure 2. Portion of a typical output voltage signal observed during the swelling process, where the gel swelling temperature is 21 °C.

min with a nitrogen purge to remove oxygen. Finally, 0.6480 g of potassium persulfate (KPS) dissolved in 40 mL of deionized water was added to start the reaction. The solution was stirred at 1000 rpm for 4 h. *N*-Isopropylacrylamide (courtesy of Kohjin Ltd., Japan) was recrystallized three times in a benzene/hexane mixture; BIS as a cross-linker was recrystallized from methanol. KPS (from Aldrich, analytical grade) as an initiator and SDS (from BDH, 99%) as a dispersant were used without further purification. In order to remove SDS, the obtained PNIPAM microgel solution was purified by successive centrifugation (15 300 rpm for 2.5 h), decantations, and dispersions in deionized water. The purified microgel solution was further concentrated to 7.5 wt % by centrifugation and decantation. The thin PNIPAM film with a thickness of 60 μm was prepared from these microgels by a high-precision quadruple film applicator. On a microscale, the film is inhomogeneous. However, the diameter of our light beam is ~ 1.5 mm and the cross-section of the light beam covers more than 10^7 particles. On the other hand, the film is much thicker than the wavelength of the light. A rough estimation shows that the light “sees” about 10^8 particles even in the expanded state. Therefore, the microscale inhomogeneities have been well averaged.

In-Situ Interferometry. As shown in Figure 1, the thin PNIPAM film was supported by a temperature-regulated optical glass plate. The top of the gel film was covered by either dry air in the drying process or by water in the swelling process. A very small fraction of the light from a Nd-YAG solid-state laser (ADLAS DPY425 II, $\lambda_0 = 532$ nm) was used as the light source. In the present setup,^{15,16} θ is very close to 0, and thus so are θ' and θ'' . Therefore, $\cos(\theta'') \sim 1$ in eq 7. The reflected light beams ($I_{R,1}$ and $I_{R,2}$) were interfered at a photodiode (Hamamatsu S2386–18K) to produce a voltage signal $V (\propto I)$. V was recorded through an analog-to-digital data acquisition system including an A/D converter (National Instruments, DAQCard-700) and a notebook computer (NEC UltraLite Versa 486SL/33).

Results and Discussion

Figure 2 shows one part of the typical observed signal in the swelling process for the thin PNIPAM gel film at 21 °C. The increase of the time interval between two neighboring minima (maxima) indicates a gradual slowing down of the swelling rate. This is expected because the elastic force inside the gel increases with swelling, while at the same time the osmotic pressure decreases. When these two forces are balanced, the gel reaches its swelling equilibrium. After correcting for the refractive index change, the signal profile in Figure 2 was transferred into the gel film thickness change (Δz) versus time (t). It should be noted that in the swelling the refractive index of the gel film (n'' in eq 7) is a function of time. For a completely dried PNIPAM film, $n'' \sim 1.5$, while for a fully swollen PNIPAM gel, $n'' \sim 1.36$. The total change of n'' is about 10%. Therefore, even if we use the average value of 1.43, the error introduced is

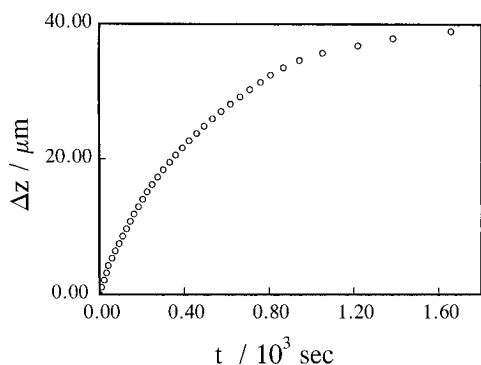


Figure 3. Typical plot of the film thickness change (Δz) versus time (t) during the swelling process at 21 °C, which is calculated on the basis of eq 7 from the signal profile shown in Figure 2.

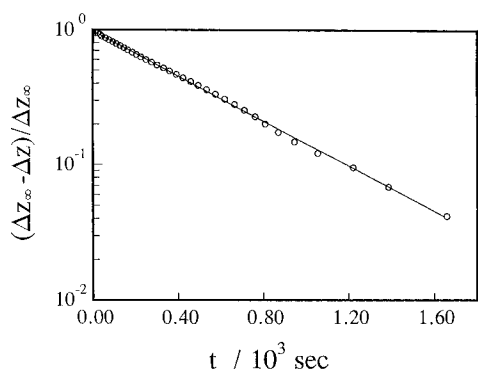


Figure 4. Typical plot of $\ln[(\Delta z_\infty - \Delta z)/\Delta z_\infty]$ versus t , where “○” are the experimental data and the continuous line represents a least-squares fitting on the basis of eq 3.

less than 5%. Practically, we measured the values of n'' at several different swelling stages to obtain an approximate calibration curve, namely, a plot of n'' versus the degree of the swelling. In this way, the error introduced by the uncertainty of n'' in the conversion of Figure 2 is no more than 1%.

Figure 3 shows a typical plot of Δz versus t for the swelling of the PNIPAM gel film at 21 °C. At $t \rightarrow \infty$, we have the maximum swelling Δz_∞ . On the basis of eq 3, B_1 and τ_1 were determined from a least-squares fitting of $\ln[(\Delta z_\infty - \Delta z)/\Delta z_\infty]$ versus t , where we have utilized the fact that the solvent uptake (W) at time t is proportional to Δz , or, in other words, $\ln[(W_\infty - W)/W_\infty] = \ln[(\Delta z_\infty - \Delta z)/\Delta z_\infty] = \ln(B_1) - t/\tau_1$.

Figure 4 shows a typical plot of $\ln[(\Delta z_\infty - \Delta z)/\Delta z_\infty]$ versus t , where “○” are experimental data and the continuous line is a least-squares fitting of $\ln[(\Delta z_\infty - \Delta z)/\Delta z_\infty]$ versus t . It shows that the swelling of the thin PNIPAM gel film follows first-order kinetics. τ_1 and B_1 were calculated from the slope and intercept of the fitting, respectively. R and D_c were further calculated from τ_1 and B_1 on the basis of eqs 4–6. It should be noted that even the initial data follow the fitting line and B_1 is close to 1, which indicates B_n ($n \geq 2$) is much smaller than B_1 since $\sum_{n=1}^{\infty} B_n = 1$. According to Li and Tanaka's theory,¹² a higher B_1 means a higher R ($=M_{\text{shear}}/M_{\text{os}}$).

Table 1 summarizes the values of B_1 , τ_1 , R , and D_c calculated from $\ln[(\Delta z_\infty - \Delta z)/\Delta z_\infty]$ versus t for the thin PNIPAM gel film swelling at different temperatures. When $T \leq 32$ °C or $T \geq 34$ °C, B_1 and R are nearly independent of T . The value of $R \sim 0.67$ is similar to that for the thin gelatin gel film,¹⁶ but significantly higher than those (~ 0.3 – 0.4) for macroscopic size gels.^{12,17} The higher R value might be related to the ultrathin thickness of the gel film. As we stated

Table 1. Summary of the Experimental Values of B_1 , τ_1 , R , and D_c for the Ultrathin PNIPAM Gel Film (60 μm) at Different Swelling Temperatures (T)

T /°C	B_1	$\tau_1/10^3\text{s}$	R	$D_c/(\text{cm}^2/\text{s})$
21.0	0.95	0.53	0.69	3.6×10^{-7}
25.0	0.93	0.81	0.67	1.5×10^{-7}
30.0	0.93	0.91	0.67	1.1×10^{-7}
32.0	0.93	0.93	0.67	7.7×10^{-8}
33.0	0.88	1.26	0.61	1.7×10^{-8}
34.0	0.86	1.38	0.57	6.3×10^{-9}
35.0	0.87	1.64	0.59	5.1×10^{-9}

before,¹⁶ for a bulk gel, water gradually diffuses from the surface into the gel. The swelling takes place first at the surface and then in the center. The surface swelling is much faster than the center swelling. This is why for bulk gels all previous swelling curves showed a very fast initial swelling process followed by a much slower first-order process. In contrast, for an ultrathin gel film, the penetration of water is nearly instantaneous. There is hardly a difference between the gel surface and the gel–glass interface. This might explain why all data points follow the first-order fitting and B_1 is higher. Table 1 shows that around the volume phase transition temperature (~ 33 °C), R has two distinct values, namely, $R \sim 0.67$ for $T < 33$ °C and $R \sim 0.58$ for $T > 33$ °C. According to its definition, $R = 1/[(K_{\text{bulk}}/M_{\text{shear}}) + 4/3]$. When T increases from below 33 °C to above, water changes from a good solvent for the gel network to a poor one. In comparison with a swollen gel network, both K_{bulk} and M_{shear} of the collapsed gel will increase. The lower R for the collapsed state means that $K_{\text{bulk}}/M_{\text{shear}}$ is relatively larger; namely, K_{bulk} increases faster than M_{shear} . Our observed T -dependence of R is consistent with the experimental results of Hirotsu obtained from a bulk PNIPAM gel wherein they directly measured osmotic bulk modulus K_{bulk} and shear modulus M_{shear} .¹⁸ For PVAC gels in *i*-PrOH, Zrinyi *et al.*¹⁷ also found that R depends on solvent quality. R decreases when a solvent becomes poor at low temperature.

Table 1 also shows that the collective coefficient (D_c) strongly depends on temperature. D_c decreased ~ 2 orders of magnitude as the gel underwent the volume phase transition. The critical slowing down of the swelling of the PNIPAM gel film was observed when T was near the transition temperature (~ 33 °C). These results are consistent with those observed in the kinetic studies of spherical PNIPAM gels.⁶ Similar results were also obtained for other gel systems.¹⁷ The values of D_c at different T are generally lower than the corresponding ones obtained for spherical gels. This agrees with the prediction that the reduction factor is directly related with the ratio of the diffusion dimensions to the total dimensions which is 3; *i.e.*, the reduction factors are 1/3 and 3/3 for an infinitely thin disk and a spherical gel.¹²

Figure 5 shows the film thickness change (Δz) during the drying process at two different temperatures (“□”: 21 °C; “△”: 25 °C) which are lower than the volume phase transition temperature (~ 33 °C). Initially, Δz was a linear function of t . Near the end of the drying, Δz decreased faster and faster until the thin film was completely dried out. This drying process is similar to that of thin gelatin films¹⁶ but does not follow the prediction for the shrinking process. According to eq 1, the decreasing rate of Δz should slow down and approach zero as time increases. This can be attributed to the fundamental difference between the drying and shrinking process. In the shrinking process, the gel is surrounded by solvent, while in the drying process the

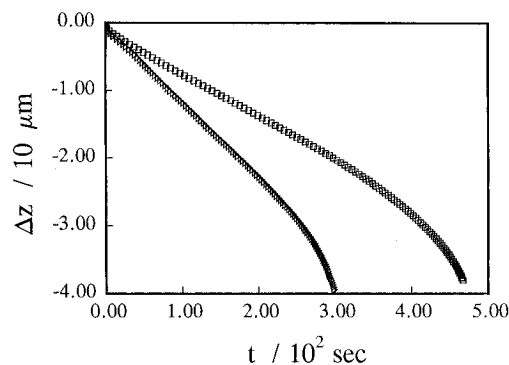


Figure 5. Typical plot of the film thickness change (Δz) versus time (t) during the drying process, where the drying temperature is 21 (\square) and 25 $^{\circ}\text{C}$ (Δ), respectively.

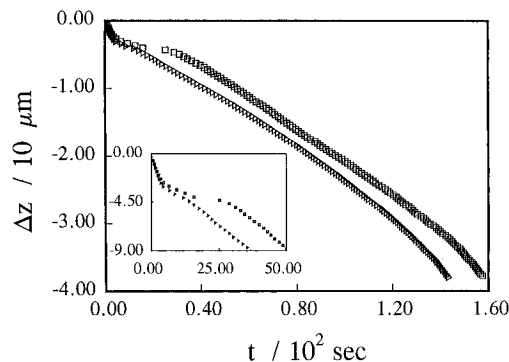


Figure 6. Typical plot of the film thickness change (Δz) versus time (t) during the drying process after temperature was jumped from the initial 25 $^{\circ}\text{C}$ to the final 33.5 (\square) and 35 $^{\circ}\text{C}$ (Δ), respectively.

gel is surrounded by dry air. Due to the effect of osmotic pressure, the diffusion of solvent from inside the gel to outside should become more and more difficult as more and more water is "squeezed" out from the gel in the shrinking process, so that the decrease of the gel thickness should slow down. However, in the drying process, the chemical potential of the solvent outside the gel is zero since there exists no solvent. Therefore, there is no extra hindering force outside to prevent the escape of solvent from the gel. The chemical potential difference for solvent inside and outside the gel is nearly a constant. This might explain why the initial decrease of Δz is a linear function of t . Near the end of the drying, the polymer segment concentration inside the gel becomes higher and higher and the film undergoes a rubber-to-glass transition, so that the interaction between the segments becomes stronger and stronger. The stronger interaction between the segments will exclude water molecules between them, which leads to a faster and faster drying.

Figure 6 shows how the PNIPAM gel film thickness change (Δz) varied with time (t) after T jumped from 25.0 $^{\circ}\text{C}$ to 33.5 and 35.0 $^{\circ}\text{C}$, respectively. The thickness change at the initial stage is much different from that under the good solvent condition shown in Figure 5 wherein the drying process is simply a water vaporization from the gel surface. However, when T is suddenly changed from 25 $^{\circ}\text{C}$ to a temperature above the volume phase transition temperature, the drying process becomes more complicated, involving at least two processes. The insert in Figure 6 shows a fast initial process (<10 s) followed by a "plateau period" and a normal drying process similar to those shown in Figure 5. The fast initial process can be attributed to the volume phase transition of the gel film, *i.e.*, shrinking. As expected, this fast process is insensitive to T as long as T is higher

than ~ 33 $^{\circ}\text{C}$. On the other hand, the drying time decreases with increasing temperature. A similar shrinking behavior was also observed for a spherical PNIPAM gel.⁷

Conclusions

The kinetics of the drying and swelling of ultrathin PNIPAM gel films can be studied by *in-situ* interferometry. In comparison with a conventional weighing or length-measuring method,^{9,10} our *in-situ* interferometry has several advantages: (1) the film thickness is much smaller than its size ($\sim 1 \times 1 \text{ cm}^2$), so that the gel film can be considered as an infinitely large disk; (2) the film thickness change can be continuously and accurately recorded by a computer; (3) due to the ultrathin thickness, the difference between the gel surface and center is much smaller than that in a bulk sample; and (4) the experimental time required to reach the final swelling equilibrium is much shorter, *i.e.*, minutes instead of hours or even days.

When the temperature is suddenly changed from 25 $^{\circ}\text{C}$ to a temperature higher than the volume phase transition temperature of PNIPAM gel, the drying involves a three-stage process, namely, a fast initial gel shrinking followed by a plateau and a normal drying process. The drying process is completely different from the gel shrinking process. Therefore, a quantitative theory is needed to describe the drying process. On the other hand, the swelling experimental results are satisfactorily represented by the swelling theory developed by Li and Tanaka. The ratio of the shear modulus (M_{shear}) over the bulk modulus (K_{bulk}) of the thin PNIPAM gel film shows two distinct values of ~ 0.67 and ~ 0.58 , respectively, for temperature below and above the volume phase transition temperature (~ 33 $^{\circ}\text{C}$). The collective diffusion coefficient (D_c) diminishes at the critical phase transition temperature. The lower values of D_c observed in this study further confirm Tanaka and Li's prediction that D_c is related to the diffusion dimension (d), namely, for an ultrathin film, $d = 1$, while for spheres, $d = 3$.

Acknowledgment. The financial support of the RGC (the Research Grants Council of the Hong Kong Government), Earmarked Grant 1994/95 (CUHK 299/94p, 221600460), is gratefully acknowledged.

References and Notes

- Schild, H. G. *Prog. Polym. Sci.* **1992**, *17*, 163 and references therein.
- Hoffman, A. S.; Afrassiabi, A.; Dong, L. C. *J. Controlled Release* **1986**, *4*, 213.
- Hoffman, A. S. *J. Controlled Release* **1987**, *6*, 297.
- Feil, H.; Bae, Y. H.; Feijen, I.; Kim, S. W. *J. Membr. Sci.* **1991**, *64*, 283.
- Osada, Y.; Ross-Murphy, S. B. *Sci. Am.* **1993**, *259*, 42.
- Tanaka, T. *Physica* **1986**, *140A*, 261.
- Matsuo, E. S.; Tanaka, T. *J. Chem. Phys.* **1988**, *89*(3), 1695.
- Park, T. G.; Hoffman, A. S. *J. Appl. Polym. Sci.* **1994**, *52*, 85.
- Yan, Q.; Hoffman, A. S. *Polymer* **1995**, *36*, 887.
- Bae, Y. H.; Okano, T.; Kim, S. W. *Pharm. Res.* **1991**, *8*, 531.
- Gutowska, A.; Bae, Y. H.; Jacobs, H.; Feijen, J.; Kim, S. W. *Macromolecules* **1994**, *27*, 4167.
- Li, Y.; Tanaka, T. *J. Chem. Phys.* **1990**, *92*(2), 1365.
- Tanaka, T.; Fillmore, D. *J. Chem. Phys.* **1979**, *70*, 1214.
- Peters, A.; Candau, S. J. *Macromolecules* **1988**, *21*, 2278.
- De Bore, J.; Visser, R. J.; Melis, G. P. *Polymer* **1992**, *33*(6), 1123.
- Wu, C.; Yan, C.-Y. *Macromolecules* **1994**, *27*, 4516.
- Zrinyi, M.; Rosta, J.; Horkay, F. *Macromolecules* **1993**, *26*, 3097.
- Hirotsu, S. *Macromolecules* **1990**, *23*, 905.